

# Rab17 regulates apical delivery of hepatic transcytotic vesicles

Anneliese C. Striz, Anna P. Stephan, Alfonso López-Coral, and Pamela L. Tuma\*

Department of Biology, The Catholic University of America, Washington, DC 20064

**ABSTRACT** A major focus for our laboratory is identifying the molecules and mechanisms that regulate basolateral-to-apical transcytosis in polarized hepatocytes. Our most recent studies have focused on characterizing the biochemical and functional properties of the small rab17 GTPase. We determined that rab17 is a monosumoylated protein and that this modification likely mediates selective interactions with the apically located syntaxin 2. Using polarized hepatic WIF-B cells exogenously expressing wild-type, dominant active/guanosine triphosphate (GTP)-bound, dominant negative/guanosine diphosphate (GDP)-bound, or sumoylation-deficient/K68R rab17 proteins, we confirmed that rab17 regulates basolateral-to-apical transcytotic vesicle docking and fusion with the apical surface. We further confirmed that transcytosis is impaired from the subapical compartment to the apical surface and that GTP-bound and sumoylated rab17 are likely required for apical vesicle docking. Because expression of the GTP-bound rab17 led to impaired transcytosis, whereas wild type had no effect, we further propose that rab17 GTP hydrolysis is required for vesicle delivery. We also determined that transcytosis of three classes of newly synthesized apical residents showed similar responses to rab17 mutant expression, indicating that rab17 is a general component of the transcytotic machinery required for apically destined vesicle docking and fusion.

## Monitoring Editor

Patrick J. Brennwald  
University of North Carolina

Received: Jul 13, 2018

Revised: Aug 31, 2018

Accepted: Sep 18, 2018

## INTRODUCTION

Unlike simple epithelial cells that directly target newly synthesized glycosphosphatidylinositol (GPI)-anchored and single transmembrane domain (TMD) proteins from the *trans*-Golgi network (TGN) to the apical membrane, hepatocytes use a more circuitous indirect

pathway (Bartles *et al.*, 1987; Bartles and Hubbard, 1988; Schell *et al.*, 1992; Ihrke *et al.*, 1998; Bastaki *et al.*, 2002; Tuma and Hubbard, 2003). In this case, newly synthesized proteins are delivered from the TGN to the basolateral surface and then selectively internalized and delivered to basolateral early endosomes. At the endosomes, the proteins are sorted into the transcytotic pathway, delivered to the subapical compartment (SAC), and finally sorted and delivered to the apical surface (Barr and Hubbard, 1993; Ihrke *et al.*, 1993; Tuma and Hubbard, 2003). A major focus of our laboratory is to identify the molecules and mechanisms that regulate transcytotic delivery of newly synthesized apical proteins in hepatocytes using polarized hepatic WIF-B cells as our model system.

WIF-B cells are an excellent hepatic model system for the study of polarized protein trafficking. They enter a terminal differentiation program, and after 7–10 d in culture, ~90% of cells are fully differentiated and exhibit polarized surface domains that are functionally and compositionally analogous to the apical and basolateral surfaces (Ihrke *et al.*, 1993; Shanks *et al.*, 1994). They display typical hepatic polarity where two adjacent cells form bile canalicular spaces that are fully sequestered from the external milieu and substratum (Ihrke *et al.*, 1993; Shanks *et al.*, 1994). Importantly for these studies, polarized protein sorting/trafficking pathways are conserved as they are in hepatocytes *in situ*. Since the late 1990s, we

This article was published online ahead of print in MBoC in Press (<http://www.molbiolcell.org/cgi/doi/10.1091/mbc.E18-07-0433>) on September 26, 2018.

The authors declare that they have no conflicts of interest with the contents of this article.

Author contributions: A.C.S. and P.L.T. are responsible for the experimental design. A.C.S., A.L.C., and A.P.S. performed all experiments. All authors analyzed and interpreted data and compiled figures. P.L.T. wrote and edited the manuscript with assistance from A.C.S. and A.L.C.

\*Address correspondence to: Pamela L. Tuma ([tuma@cua.edu](mailto:tuma@cua.edu)).

Abbreviations used: 5'NT, 5' nucleotidase; APN, aminopeptidase N; ASGP-R, asialoglycoprotein receptor; EEA1, early endosomal antigen 1; FBS, fetal bovine serum; GAP, GTPase-activating protein; GDI, GDP dissociation inhibitor; GEF, guanine nucleotide exchange factor; HCC, hepatocellular carcinoma; MRP2, multidrug associated protein-2; plgA-R, polymeric immunoglobulin A receptor; SAC, subapical compartment.

© 2018 Striz *et al.* This article is distributed by The American Society for Cell Biology under license from the author(s). Two months after publication it is available to the public under an Attribution–Noncommercial–Share Alike 3.0 Unported Creative Commons License (<http://creativecommons.org/licenses/by-nc-sa/3.0>).

“ASCB®,” “The American Society for Cell Biology®,” and “Molecular Biology of the Cell®” are registered trademarks of The American Society for Cell Biology.

and our colleagues have characterized WIF-B endocytic and biosynthetic pathways and mapped out the itineraries of recycling receptors, apical and basolateral residents (Tuma *et al.*, 1999, 2001; Tuma and Hubbard, 2001, 2003; Nyasae *et al.*, 2003), and have developed many useful assays for specifically monitoring hepatic protein trafficking (Ihrke *et al.*, 1998; Tuma *et al.*, 2001, 2002; Ramnarayanan *et al.*, 2007; In *et al.*, 2012, 2014). With such assays in hand, the WIF-B cells have been used as surrogates for normal hepatocytes by us and others in studies of protein trafficking and other fundamental hepatic processes in liver health (Meads and Schroer, 1995; Chaumontet *et al.*, 1998; Alvarez *et al.*, 1999; Hayes *et al.*, 1999; Sturm *et al.*, 2000; Lionne *et al.*, 2001; Neufeld *et al.*, 2002; Gradilone *et al.*, 2005; Wakabayashi *et al.*, 2005; Harder *et al.*, 2007; Paulusma *et al.*, 2008; Suda *et al.*, 2015) and disease (Graf *et al.*, 2003; Schaffert *et al.*, 2004; Garuti *et al.*, 2005; Biagini *et al.*, 2006; Folmer *et al.*, 2009; Gao *et al.*, 2009; McVicker *et al.*, 2009, 2012; Leitch *et al.*, 2010; Pujol *et al.*, 2011; Nyasae *et al.*, 2014).

Our most recent studies have focused on characterizing the biochemical and functional properties of the low-molecular-weight rab17 GTPase. In the mid-1990s, rab17 was identified as a polarized epithelia-specific rab isoform with enriched expression in liver, kidney, and intestine (Lutcke *et al.*, 1993; Lehtonen *et al.*, 1999). Its subapical distributions in many different cell types and tissues (Lutcke *et al.*, 1993; Hunziker and Peters, 1998; Zacchi *et al.*, 1998; Peters and Hunziker, 2001), its copurification with hepatic transcytotic vesicles (Jin *et al.*, 1996), and our findings from split ubiquitin yeast two-hybrid screens that rab17 binds myelin and lymphocyte protein 2 (MAL2; a known regulator of hepatic transcytosis) (De Marco *et al.*, 2002; In and Tuma, 2010) have all implicated rab17 as a regulator of transcytosis. A role for rab17 in transcytosis has been confirmed from studies in polarized mammary gland-derived Eph4 cells and in Madin–Darby canine kidney (MDCK) cells (Hunziker and Peters, 1998; Zacchi *et al.*, 1998) but with conflicting results. Overexpression of wild-type (WT) rab17 was found to *impair* basolateral-to-apical transcytosis in MDCK cells, whereas overexpression of the dominant active or dominant negative rab17 *enhanced* transcytosis in the same direction in Eph4 cells (Hunziker and Peters, 1998; Zacchi *et al.*, 1998). Despite the enriched rab 17 expression in the liver, such transcytosis studies have not been performed in polarized hepatocytes.

More recently, rab17 expression has been detected in hippocampus and in melanocytes (Beaumont *et al.*, 2011; Mori *et al.*, 2012). Functional studies using hippocampal neurons indicate that rab17 mediates cargo delivery to developing dendrites and dendritic spines, thereby regulating dendrite formation (Mori *et al.*, 2012). In melanocytes, rab17 knockdown led to increased intracellular melanin without corresponding changes in melanosome maturation or movement. Because filipodia (the putative melanin release sites) formation was also impaired, the authors concluded that increased melanin content is due to impaired melanosome fusion (Beaumont *et al.*, 2011). These newer findings additionally implicate rab17 as a mediator of membrane fusion with the cell surface. Thus, we hypothesize that rab17 functions in hepatic transcytotic vesicle docking and fusion at the apical membrane by interacting with the soluble *N*-ethylmaleimide-sensitive factor activating protein receptor (SNARE)-mediated machinery. This hypothesis is further supported by our recent findings that rab17 specifically interacts with the apically located syntaxin 2 but not syntaxin 3 (also apically located) or syntaxin 4 (basolaterally located) (Striz and Tuma, 2016).

To directly test our hypothesis that rab17 mediates hepatic transcytotic vesicle docking and fusion at the apical membrane, we

monitored the basolateral-to-apical transcytosis of three classes of newly synthesized apical residents including 5' nucleotidase (5'NT) (GPI-anchored), aminopeptidase N (APN; single TMD integral membrane protein), and polymeric IgA-receptor (plgA-R; a "professional" transcytosing protein) in cells expressing wild-type, guanosine triphosphate (GTP)-bound/Q77L, guanosine diphosphate (GDP)-bound/N132I, and sumo-deficient/K68R rab17. Our data confirm a role for rab17 in regulating hepatic basolateral-to-apical transcytosis and implicate that rab17 sumoylation and GTP hydrolysis are required for docking and fusion of hepatic transcytotic vesicles from the SAC to the apical surface. Because rab17 has been implicated as a tumor suppressor in the progression of human hepatocellular carcinoma (Qi *et al.*, 2015; Wang *et al.*, 2015), these results are clinically significant and may lead to the development of novel therapeutic strategies.

## RESULTS

### Rab17 regulates basolateral-to-apical transcytosis in polarized hepatocytes

In Figure 1A, the typical, polarized hepatic morphology of the terminally differentiated WIF-B cells is shown. The phase lucent structures formed between two cells are functionally and compositionally analogous to bile canaliculi that are fully sequestered from the external milieu with tight junctions separating them from the basolateral domain. To first determine whether overexpression of wild-type rab17 impairs hepatic transcytosis as observed in MDCK cells, we monitored the constitutive basolateral-to-apical trafficking of three classes of newly synthesized apical residents: 5'NT (GPI-anchored), APN (single TMD), and plgA-R ("professional" transcytotic cargo, i.e., a protein that transcytoses in all epithelial cell types) in control (uninfected) or wild-type rab17-expressing cells as we have described (Ihrke *et al.*, 1998; Ramnarayanan *et al.*, 2007; In and Tuma, 2010; In *et al.*, 2012; Groebner *et al.*, 2014). As we have previously shown, wild-type rab17 is detected as both a 25-kDa and a 40-kDa monosumoylated species (Figure 1B) (Striz and Tuma, 2016).

Live cells were basolaterally labeled with antibodies specific to external epitopes of the apical proteins for 20 min at 4°C. The cells were rewarmed to 37°C, the antibody-antigen complexes were chased to the apical surface for either 90 min (for 5'NT) or 60 min (for APN and plgA-R) and the cells were fixed and processed for indirect immunofluorescence detection of the trafficked proteins. Because tight junctions restrict antibody access to the apical surface, only basolateral labeling was detected after 0 min of chase in control (uninfected) or rab17-expressing cells (Figure 1C; unlabeled bile canalicular spaces are marked with asterisks). After chase, robust and discrete apical labeling was observed in both control (uninfected) cells or cells expressing wild-type rab17 for all three proteins (secretory component is not cleaved from plgA-R in WIF-B cells [Ihrke *et al.*, 1998; Bastaki *et al.*, 2002]) with a reciprocal loss of basolateral labeling indicating successful apical delivery (Figure 1C). To confirm the morphological observations, we measured apical delivery by measuring the relative fluorescence intensities of each marker at the apical versus basolateral surface after the indicated times of chase as we have described (Ramnarayanan *et al.*, 2007; In and Tuma, 2010; In *et al.*, 2012, 2014; Groebner *et al.*, 2014). As shown in Figure 1D, similar levels of apical delivery were observed for all three markers in control and infected cells, indicating that overexpression of wild-type rab17 did not impair transcytosis as observed in MDCK cells.

To determine whether hepatic transcytosis exhibited similar rab17 nucleotide dependence as observed in polarized Eph4 cells (Zacchi *et al.*, 1998), we monitored apical delivery of the same set of newly synthesized apical proteins in cells expressing wild-type,

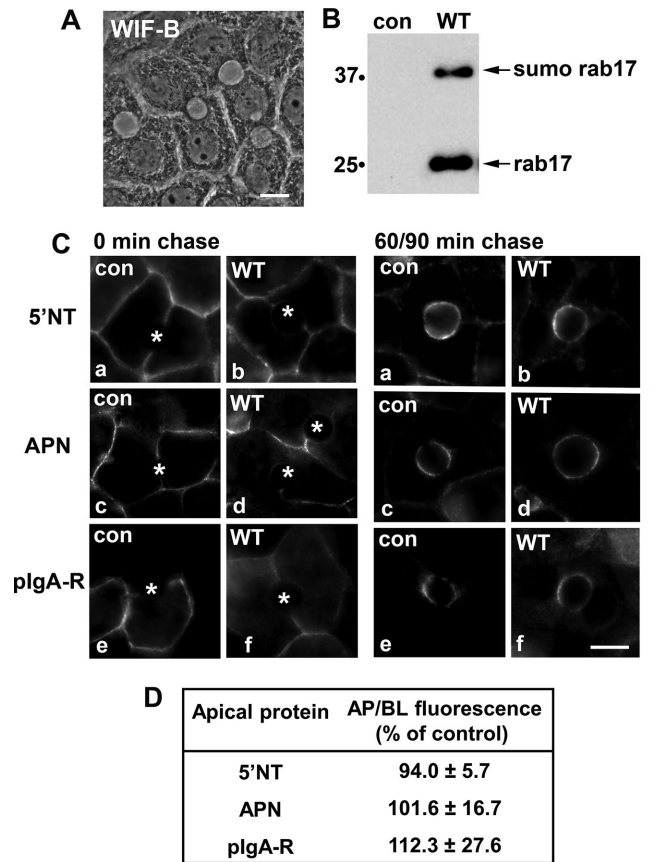


**FIGURE 1:** Basolateral-to-apical transcytosis is not altered by overexpression of wild-type rab17. (A) The characteristic, polarized hepatic morphology of WIF-B cells is shown in a phase image. (B) Total cell lysates were prepared from uninfected (control) WIF-B cells or cells expressing FLAG-tagged WT rab17 and immunoblotted with anti-FLAG antibodies. The monosumoylated form of rab 17 is indicated (sumo rab17). Molecular weight markers are indicated on the left of each immunoblot in kDa. (C) Uninfected cells or cells expressing wild-type rab 17 were basolaterally labeled with antibodies specific for the extracellular epitopes of the indicated apical proteins at 4°C. Cells were additionally infected with recombinant adenoviruses expressing plgA-R in panels e and f (C). After excess antibodies were washed away, antibody-antigen complexes were chased for 0, 90, or 60 min as indicated at 37°C. Cells were fixed, permeabilized, and labeled with secondary antibodies to detect the transcytosed proteins. Asterisks mark the unlabeled bile canaliculi. Images are representative of at least three experiments. Bar = 10 μm. (D) Control (uninfected) WIF-B cells or cells expressing wild-type rab17 were basolaterally labeled for the indicated apical proteins and chased as described in C. Random fields were visualized by indirect immunofluorescence. From micrographs, the average pixel intensity of each marker at selected regions of interest placed at the apical or basolateral membrane of the same WIF-B cell was measured. The averaged background pixel intensity was subtracted from each value and the ratio of apical- (ap) to-basolateral (bl) fluorescence intensity was determined. Wild-type values were normalized to control values that were set to 100%. Values are expressed as the mean ± SEM. Measurements were performed on at least three independent experiments.

GTP-bound/Q77L, or GDP-bound/N132I rab17. As we have previously shown, both the 25-kDa and 40-kDa rab17 species were detected in cells expressing wild-type or mutant rab17 (Figure 2A). As we have also shown previously, sumoylation on the N132I mutant is

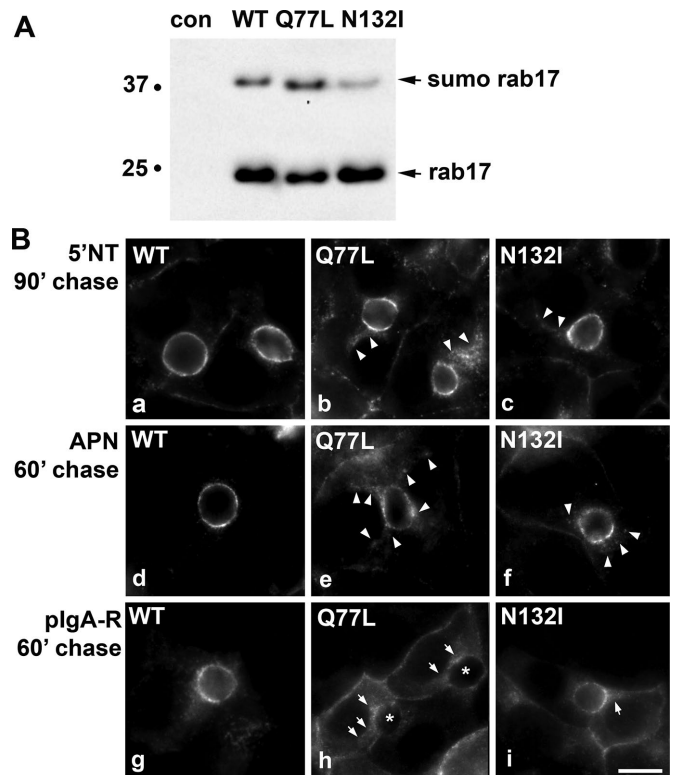


**FIGURE 2:** Transcytosis is impaired in cells expressing GTP-bound/Q77L or GDP-bound/N132I rab17. (A) Total cell lysates were prepared from WIF-B cells expressing FLAG-tagged WT, GTP-bound/Q77L, or GDP-bound/N132I rab17 and immunoblotted with anti-FLAG antibodies. The monosumoylated form of rab 17 is indicated (sumo rab17). Molecular weight markers are indicated on the left of each immunoblot in kDa. (B) Cells expressing wild-type, GTP-bound/Q77L, or GDP-bound/N132I rab17 were basolaterally labeled with antibodies specific for the extracellular epitopes of the indicated apical proteins at 4°C. Cells were additionally infected with recombinant adenoviruses expressing plgA-R in panels g–i. After excess antibodies were washed away, antibody-antigen complexes were chased for 90 min (a–c) or 60 min (d–i) at 37°C. Cells were fixed, permeabilized, and labeled with secondary antibodies to detect the transcytosed proteins. Arrows indicate subapically accumulated transcytosing proteins in cells expressing mutant rab17. Images are representative of at least three experiments. Bar = 10 μm.

more variable, and in this example is somewhat decreased (Striz and Tuma, 2016). Opposite of what was observed in Eph4 cells, expression of both the dominant negative/N132I and dominant active/Q77L rab17 led to the subapical accumulation of all three classes of chased apical proteins (Figure 2B). When quantitated, the dominant negative rab17 led to a significant 30–50% impairment in apical delivery compared with cells expressing wild-type rab17, whereas the expression of the dominant active/Q77L rab17 led to an even greater impairment (ranging from ~45% to 60%) of the three chased proteins relative to wild type (Figure 3). Together these results suggest that rab17 function in transcytosis varies among polarized epithelial cell types (see Discussion). The observed impairment and subapical accumulation of the chased transcytotic cargo in cells expressing mutant rab17 further suggest that in hepatocytes, rab17 regulates apical delivery from the SAC and that vesicle delivery is not only nucleotide dependent but also may require GTP hydrolysis (see Discussion).

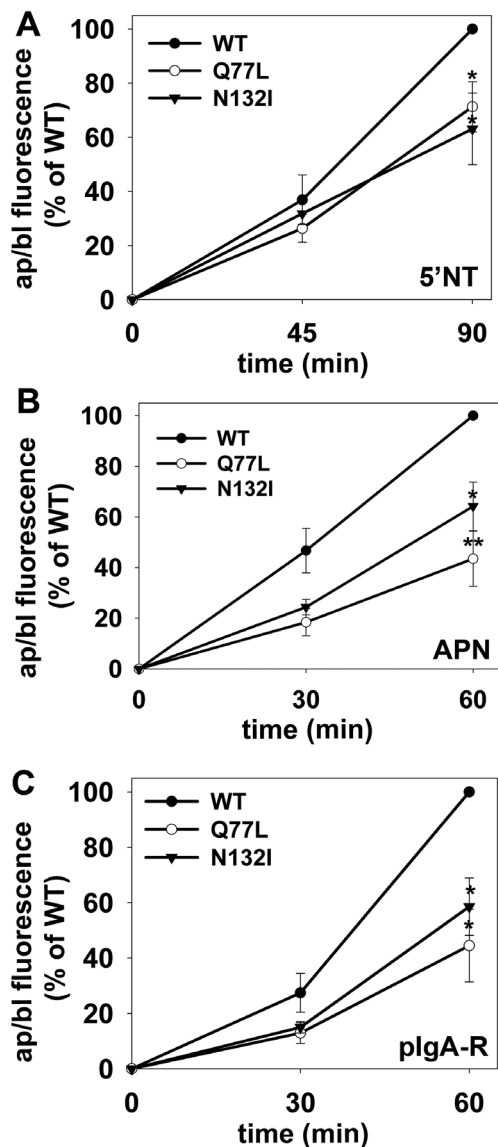


**FIGURE 3:** Transcytosis is impaired to a similar extent for different classes of apical proteins in cells expressing GTP-bound/Q77L or GDP-bound/N132I rab17. WIF-B cells expressing wild-type, GDP-bound/Q77L, or GDP-bound/N132I rab17 were basolaterally labeled for the indicated apical proteins as described in Figure 2 and chased for 0, 45, or 90 min (A) or 0, 30, or 60 min (B, C) at 37°C. Cells were additionally infected with recombinant adenoviruses expressing plgA-R in C. Cells were fixed, permeabilized, and labeled with secondary antibodies to detect the transcytosed proteins. Random fields were visualized by indirect immunofluorescence and digitized. From micrographs, the average pixel intensity of each marker at selected regions of interest placed at the apical or basolateral membrane of the same WIF-B cell was measured. The averaged background pixel intensity was subtracted from each value and the ratio of apical (ap) to basolateral (bl) fluorescence intensity was determined. Values are expressed as the mean  $\pm$  SEM for 5'NT (A), APN (B), and plgA-R (C) and are from at least three independent experiments. \* $p \leq 0.05$ , \*\* $p \leq 0.005$ .

### Rab17 regulates transcytotic vesicle delivery from the SAC to the apical surface

From our previous studies, we determined that expression of GTP-bound/Q77L led to the steady-state redistribution of 5'NT and

syntaxin 2 into the same subapical structures (Striz and Tuma, 2016). To determine whether the subapical structures that accumulated transcytosing apical proteins were also positive for syntaxin 2, we immunolabeled cells expressing GTP-bound/Q77L for steady-state syntaxin 2 distributions vs. 5'NT chased for 90 min. In uninfected control cells, both syntaxin 2 and trafficked 5'NT colocalized at the apical surface (Figure 4A). As predicted, transcytosing 5'NT accumulated in syntaxin 2-positive, subapical structures in Q77L rab17-expressing cells (arrowheads) with a Mander's coefficient of  $0.77 \pm 0.03$ , confirming a high degree of colocalization (Figure 4A).

The extreme proximity of the apical structures to the apical surface implies the transcytosing apical residents were derived from or are present in the SAC. To confirm this prediction, we monitored colocalization of trafficked apical residents with markers of the two hepatic transcytotic intermediates (basolateral early endosomes and SAC) (Tuma and Hubbard, 2003) and with a marker for apical endosomes. To first rule out that the structures were basolateral early endosomes (the first transcytotic intermediate encountered after basolateral internalization; Tuma and Hubbard, 2003), we monitored cotrafficking of basolaterally internalized 5'NT with asialoglycoprotein receptor (ASGP-R). After 60 min of chase, no overlap between the two proteins was observed in control (uninfected) cells as expected (Figure 4B), which was confirmed by a low Mander's coefficient of colocalization ( $0.07 \pm 0.01$ ) (Figure 4F). No colocalization was observed in cells expressing GTP-bound/Q77L (Figure 4B) with Mander's coefficients nearly identical to control ( $0.08 \pm 0.01$ ), confirming the compartments with accumulated apical proteins are not basolateral early endosomes. To rule out accumulation in apical endosomes, we colabeled basolaterally internalized APN with steady-state early endosomal antigen 1 (EEA1). The characteristic punctate staining for EEA1 that we have described previously (Tuma *et al.*, 2001) was observed in uninfected and the rab mutant expressing cells (Figure 4C). Merged images reveal no colocalization between EEA1 and APN. This was further confirmed with low Mander's coefficients determined for control ( $0.15 \pm 0.03$ ) that were not changed in cells expressing Q77L rab17 ( $0.15 \pm 0.01$ ) (Figure 4F).

To confirm that the subapical puncta are derived from or are present in the SAC, we cotrafficked basolaterally internalized APN and endolyn-78 (Figure 4D). Although at steady-state endolyn-78 is a lysosomal resident, basolaterally retrieved endolyn-78 populations are delivered to the SAC en route to lysosomes (Ihrke *et al.*, 1998). This itinerary allows us to specifically identify the SAC by monitoring the distribution of basolaterally internalized endolyn-78 after 60 min of chase as described (Ihrke *et al.*, 1998). In uninfected control cells, APN localized mainly to the apical surface after 60 min of chase with only a small detectable overlap with endolyn-78 located in the SAC. A low-to-moderate Mander's coefficient of  $0.19 \pm 0.01$  confirmed this observation (Figure 4F). In contrast, in GTP-bound/Q77L rab17-expressing cells, the subapically accumulated APN labeling significantly overlapped with endolyn-78 in the SAC (Figure 4D). Additionally, the Mander's coefficients increased approximately threefold in the mutant-expressing cells to  $0.66 \pm 0.02$  (Figure 4F) confirming that the identity of the subapical structures as the SAC. For control, we monitored the steady-state distributions of the three markers in cells expressing wild-type or GTP-bound/Q77L rab17. As shown in Figure 4E, the steady-state distributions of ASGP-R, endolyn-78, and EEA1 did not change in cells expressing Q77L rab17 (or K68R rab17; see Figure 6 later in this article), confirming their suitability as specific compartment markers in mutant-expressing cells. From these results, we conclude that rab17 mediates vesicle docking and fusion from the SAC to the apical surface and that this process is GTP dependent (see *Discussion*).

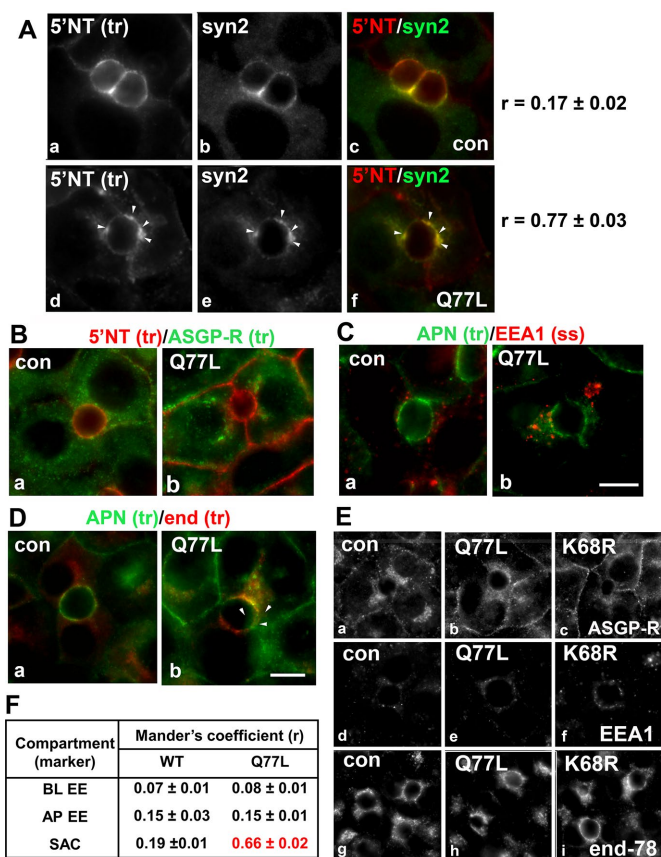


**FIGURE 4:** Transcytosing proteins accumulate in syntaxin 2–positive SAC structures in cells expressing GTP-bound/Q77L rab17. (A) Control (uninfected) WIF-B cells or cells expressing GTP-bound/Q77L rab17 were basolaterally labeled with antibodies against 5'NT and antigen-antibody complexes were chased for 60 min. Cells were fixed and double labeled for steady-state syntaxin 2 distributions. Merged images are shown in panels c and f. Arrows indicate subapically accumulated transcytosing proteins in cells expressing mutant rab17. Bar = 10  $\mu$ m. Mander's coefficients of colocalization are indicated on the right. Values are expressed as the mean  $\pm$  SEM from at least three independent experiments. Control (uninfected) WIF-B cells or cells expressing GTP-bound/Q77L rab17 were basolaterally labeled for 5'NT and ASGP-R (B) or APN (C) or APN and endolyn-78 (D) and allowed to continuously chase for 60 min. Cells were fixed and stained for the corresponding trafficked antibody–antigen complexes. In C, cells were labeled for steady-state distributions of EEA1. Merged images are shown for each. Arrows indicate subapically accumulated transcytosing proteins in cells expressing mutant rab17. Bar = 10  $\mu$ m. In E, control (uninfected) WIF-B cells or cells expressing GTP-bound/Q77L or sumo-deficient/K68R rab17 were labeled for the steady-state distributions of ASGP-R, EEA1, and endolyn-78 as indicated. No changes in distributions were observed for any of the proteins confirming the validity of their use as compartment markers. Bar = 10  $\mu$ m. In F, Mander's coefficients of colocalization for the experiments shown in B, C, and D are shown. Values are expressed as the mean  $\pm$  SEM from at least three independent experiments. BL EE, basolateral early endosome; AP EE, apical early endosome; SAC, subapical compartment.

### Rab17 monosumoylation is required for optimal apical delivery

To determine whether rab17 sumoylation is required for rab17 function in transcytosis, we monitored the constitutive basolateral-to-apical trafficking of the same set of newly synthesized proteins in

cells expressing a sumo-deficient rab17 mutant (K68R). As observed for cells expressing the GTP/GDP-bound rab17 mutants, robust basolateral labeling of all three markers was observed at 0 min of chase in cells expressing K68R rab17 (Figure 5, A, C and E). After chase, all three trafficked proteins were all detected in subapical structures (Figure 5, A, C and E), indicating a similar block in trafficking from the SAC to the apical surface. When quantitated, there was a significant decrease in delivery for all three classes of apical residents in sumo-deficient/K68R rab17-expressing cells. When compared with uninfected control cells, APN and 5'NT transcytosis was impaired by ~50% in K68R-expressing cells ( $50.4 \pm 9.4\%$  and  $55.4 \pm 8.3\%$  of control, respectively) (Figure 5, B and D). Delivery of plgA-R was impaired to even a greater extent to only  $39.2 \pm 8.0\%$  of control (Figure 5F).

Because sumoylation is decreased by ~30% in the K68R mutant (Figure 6A) (Striz and Tuma, 2016) and in (Figure 6A) rab17. We next monitored transcytosis in cells treated with anacardic acid, an inhibitor of the first step of the three-step sumoylation process. Cells were pretreated with 5  $\mu$ M anacardic acid for 60 min at 37°C before antibody labeling, and the assay was performed in the continued presence of the drug, conditions we established previously that led to a significant decrease in wild-type rab17 sumoylation by ~60%, a twofold-greater decrease than observed for the K68R mutant. (Striz and Tuma, 2016). As for cells expressing K68R rab17, the subapical accumulation of transcytosing proteins was observed in treated cells (Figure 6B), and when quantitated, delivery was impaired to  $50.1 \pm 6.1\%$  of control. In cells expressing K68R rab17 that were additionally treated with anacardic acid, no further decrease (55% of control) in apical delivery was observed (unpublished data). This result coupled with the remarkable similarity in values for the K68R- and anacardic acid-induced impairment in apical delivery further suggest that lysine 68 is the major, functional sumoylated residue in rab17 (see Discussion).

To confirm that K68R rab17 impaired transcytosis at the same step as expression of the Q77L rab17, we first determined whether the subapical structures that accumulated transcytosing apical proteins were also positive for syntaxin 2. As predicted, transcytosing 5'NT accumulated in syntaxin 2–positive, subapical structures in K68R rab17-expressing cells (arrowheads) with a relatively high Mander's coefficient of colocalization ( $0.54 \pm 0.04$ ) (Figure 6C). Also as seen in cells expressing Q77L rab17, no colocalization of trafficking proteins was observed with the basolateral early endosomes ( $r = 0.07 \pm 0.01$ ) (Figure 6D, a) or apical early endosomes ( $r = 0.11 \pm 0.02$ ) (Figure 6D, b), whereas a high degree of colocalization was observed with the SAC marker ( $r = 0.57 \pm 0.04$ ) (Figure 6D, c). As shown in Figure 4E, the steady-state distributions of ASGP-R, endolyn-78, and EEA1 did not change in cells expressing or K68R rab17, confirming their suitability as specific compartment markers in mutant-expressing cells. To better model rab17 function in transcytosis (see Discussion), we determined whether both the 25- and 40-kDa rab17 species could bind GTP, we performed GTP pull downs. As shown in Figure 6E, both the 25-kDa rab17 and the 40-kDa monosumoylated rab17 species from both wild-type and the K68R mutant proteins bound GTP. Thus, we conclude that sumoylated rab17 is required for optimal syntaxin 2–mediated, GTP-dependent apical vesicle docking and fusion (see Discussion).

### Rab17 selectively regulates transcytosis

To determine whether rab17 selectively regulates apical protein delivery, we examined constitutive basolateral secretion and basolateral delivery of newly synthesized plgA-R, two transport steps regulated by MAL2, a rab17 binding partner (In and Tuma, 2010;

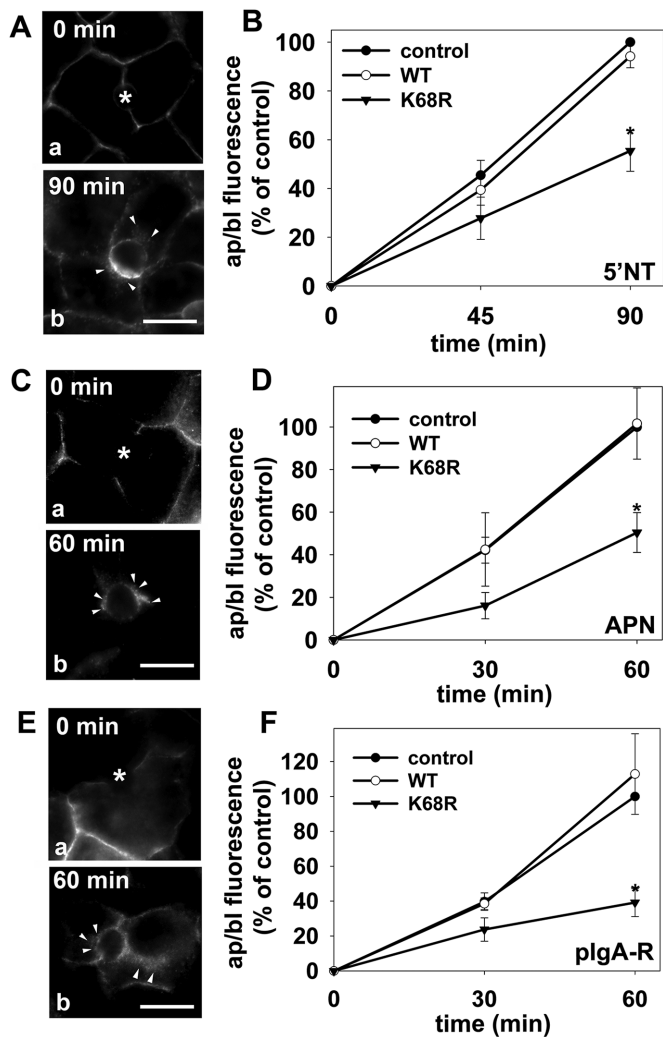


**FIGURE 5:** Transcytosis is impaired to a similar extent for different classes of apical proteins in cells expressing sumo-deficient/K68R rab17. (A–F) Control (uninfected) cells and cells expressing wild-type or sumo-deficient/K68R rab17 were basolaterally labeled with antibodies specific for the extracellular epitopes of the indicated apical proteins at 4°C. Cells were additionally infected with recombinant adenoviruses expressing plgA-R in E and F. After excess antibodies were washed away, antibody–antigen complexes were chased for 0, 60 min, or 90 min as indicated (A, C, and E) at 37°C. Cells were fixed, permeabilized and labeled with secondary antibodies to detect transcytosed APN (A), 5'NT (C) or plgA-R (E). Asterisks are marking unlabeled canaliculi. Images are representative of at least three experiments. Bar = 10  $\mu$ m. (B, D, F) Control (uninfected) WIF-B cells or cells expressing wild-type or sumo-deficient/K68R rab17 were basolaterally labeled for the indicated apical proteins as described in Figure 1 and chased for 0, 45, or 90 min (B) or 0, 30 or 60 min (D and F) at 37°C. Cells were fixed, permeabilized, and labeled with secondary antibodies to detect the transcytosed proteins. Random fields were visualized by indirect immunofluorescence. From micrographs, the average pixel intensity of each marker at selected regions of interest placed at the apical or basolateral membrane of the same WIF-B cell was measured. The averaged background pixel intensity was subtracted from each value, and the ratio of apical (ap) to basolateral (bl) fluorescence intensity was determined. Values are expressed as the mean  $\pm$  SEM for 5'NT (B), APN (D), and plgA-R (F). Measurements were performed on at least three independent experiments. \* $p$   $\leq$  0.05.

In *et al.*, 2014). To monitor secretion, we measured albumin release into the culture medium by immunoblotting. As shown in Figure 7A, similar levels of secreted albumin were detected in cells expressing wild-type or mutant rab17, and, when quantitated, overlapping kinetics were observed (Figure 7B). To monitor TGN-to-basolateral membrane delivery of newly synthesized plgA-R, we used a method we previously described (Ramnarayanan *et al.*, 2007) where the basolaterally labeled population of the receptor is normalized to total plgA-R expressed. As shown in Figure 7C, cells expressing wild-type or mutant rab17 showed similar ratios of basolateral-to-total plgA-R, indicating that basolateral delivery was not changed. For comparison, we monitored basolateral delivery of newly synthesized APN. Although a decrease was observed in the basolateral population of APN in cells expressing GDP-bound/N132I rab17, this was not significant. Importantly, rab17 expression did not alter expression levels of either APN or plgA-R (Figure 7D). Finally, we monitored the steady-state distributions of the basolateral resident protein, HA321, in rab17-expressing cells. As shown in Figure 7E, HA321 expression was tightly restricted to the basolateral surface with no intracellular/TGN labeling observed in cells expressing wild-type, GTP-bound/Q77L, or GDP-bound/N132I rab17. Together these results indicate rab17 selectively regulates hepatic transcytotic apical delivery.

## DISCUSSION

We have confirmed that rab17 regulates basolateral-to-apical transcytosis at the last step from the SAC to the apical surface in polarized hepatocytes. We further conclude that rab17 regulates apical vesicle docking and fusion via interactions with syntaxin 2 and that maximal docking is achieved when rab17 is sumoylated and GTP-bound. Additionally, we propose that GAP-activated GTP hydrolysis is required for vesicle fusion with the apical membrane (see below). Because trafficking of all three classes of apical residents examined showed similar responses to rab17 mutant expression, we conclude that rab17 is a general component of the transcytotic machinery required for apically destined vesicle docking and fusion.

## Our working model

On the basis of our initial characterization of rab17 sumoylation and the results presented here, we have constructed a working model for rab17 function in apical vesicle docking and fusion (Figure 8). We propose that the prenylated, monosumoylated, and GDP-bound rab17 is activated by its specific guanine nucleotide exchange factor (GEF) at the SAC allowing associations with a budding vesicle through interactions with a transcytotic vesicle-associated membrane protein (VAMP) or yet-to-be-identified coat component (unpublished data). At the apical surface, monosumoylated, GTP-bound rab17 mediates vesicle docking via specific interactions with syntaxin 2. Somewhat surprisingly, we determined that expression of the GTP-bound rab17 led to the subapical accumulation of transcytotic cargo. Because rab17 is sumoylated and GTP-bound when associated with syntaxin 2 (Striz and Tuma, 2016) and because wild-type rab17 expression does not alter apical delivery, the simple prediction is that GTP hydrolysis is required for fusion such that expression of the GTP-bound, hydrolysis-deficient rab17 prevents vesicle delivery. This would explain the subapical accumulation of apical vesicles either just adjacent to or docked at the apical surface in Q77L/GTP-bound rab17-expressing cells. The codistribution of syntaxin 2 with the stalled, rab17-positive vesicles implicates the latter possibility. Nonetheless, we propose rab17 encounters its specific GAP at the apical membrane after vesicle docking thereby activating GTP hydrolysis leading to vesicle fusion. Alternatively

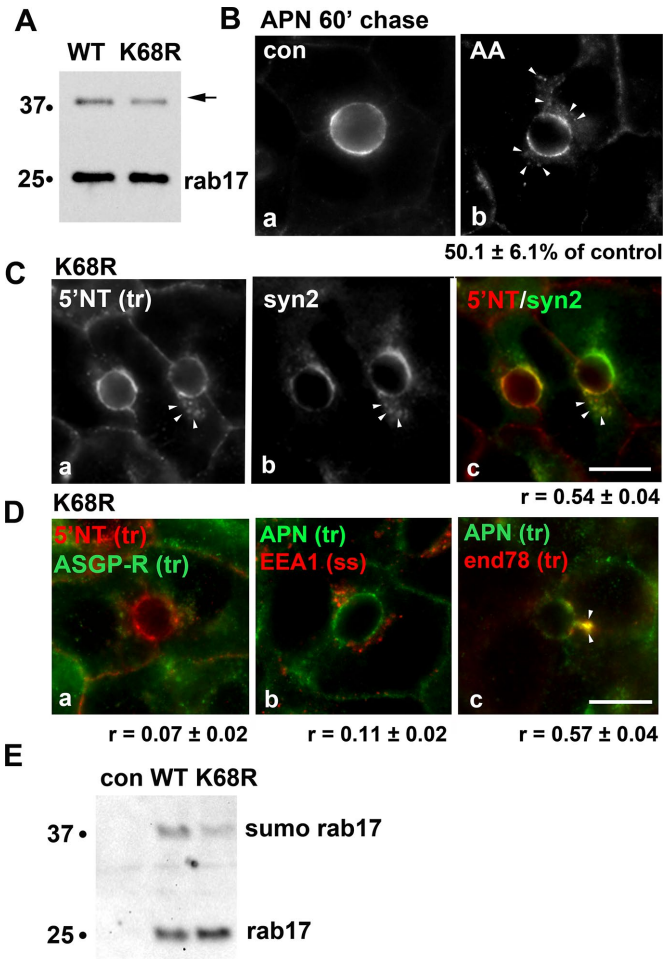


**FIGURE 6:** Transcytosing proteins accumulate in syntaxin 2-positive SAC structures in cells expressing sumo-deficient rab17. (A) Total cell lysates were prepared from WIF-B cells expressing FLAG-tagged WT or sumo-deficient/K68R rab17 and immunoblotted with anti-FLAG antibodies. The mono-sumoylated form of rab17 is indicated with an arrow. Molecular-weight markers are indicated on the left of each immunoblot in kDa. (B) Uninfected WIF-B cells were pretreated with 5  $\mu$ M anacardic acid (AA) for 60 min at 37°C before APN antibody labeling at 4°C for 20 min. APN-antibody complexes were chased for 60 min in the continued presence of the drug. The amount of impaired transcytosis is indicated below the panel as the percent of control. Values are expressed as the mean  $\pm$  SEM from at least three independent experiments. (C) WIF-B cells expressing sumo-deficient/K68R rab17 were basolaterally labeled with antibodies against 5'NT, and antigen-antibody complexes were chased for 60 min. Cells were fixed and double labeled for steady-state syntaxin 2 distributions. A merged image is shown in panel c. Arrows indicate subapically accumulated transcytosing proteins in cells expressing mutant rab17. Bar = 10  $\mu$ m. The Mander's coefficient of colocalization is indicated below the merged image. Values are expressed as the mean  $\pm$  SEM from at least three independent experiments. (D) WIF-B cells expressing sumo-deficient/K68R rab17 were basolaterally labeled for 5'NT and ASGP-R (a) or APN (b) or APN and endolyn-78 (c) and allowed to continuously chase for 60 min. Cells were fixed and stained for the corresponding trafficked antibody-antigen complexes. In D (panel b), cells were labeled for steady-state distributions of EEA1. Merged images are shown. Arrows indicate subapically accumulated transcytosing proteins in cells expressing mutant rab17. Mander's coefficients of colocalization are indicated below. Values are expressed as the mean  $\pm$  SEM from at least three independent experiments. Bar = 10  $\mu$ m. (E) Uninfected WIF-B cells (con) or cells expressing WT of K68R rab16 were lysed in ice-cold GTP binding

(unpublished data), rab17 GTPase activity may catalyze its release from the SNARE machinery and subsequent associations with a GDP dissociation inhibitor. In either case, the GDP-bound rab17 is escorted back to the SAC by a GDP dissociation inhibitor (GDI) for another round of vesicle budding.

To fully test this model, it will be important to identify the rab17-specific GEF and GAP. Rab17 is a member of the rab5 subfamily of

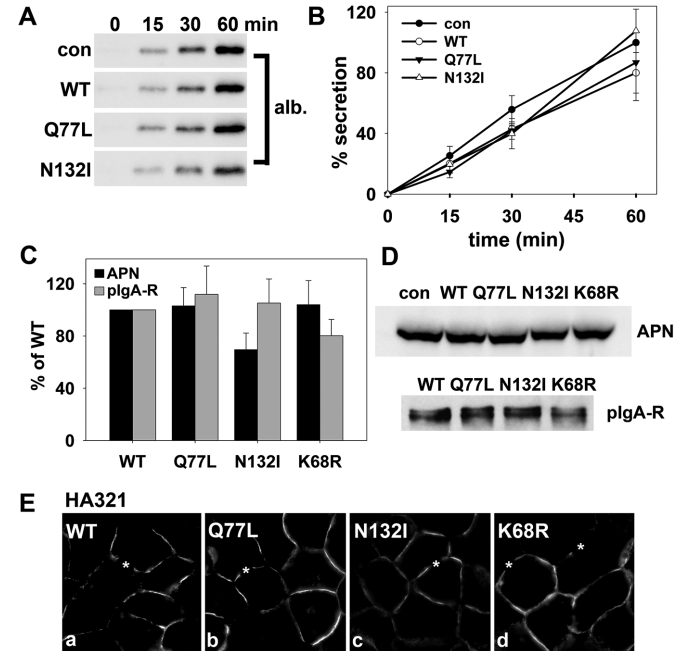


**FIGURE 7:** Rab17 selectively regulates transcytosis. (A, B) Control (uninfected) cells or cells expressing wild-type, GTP-bound/Q77L, or GDP-bound/N132I rab17 were washed in PBS and reincubated in serum-free medium. At 0, 15, 30, and 60 min after reincubation, aliquots of media were collected and immunoblotted for albumin (A). Densitometric analysis of the immunoreactive species was performed and albumin secretion plotted as a percentage of control at 60 min (B). Values are expressed as the average  $\pm$  SEM from at least three independent experiments. (C) Cells expressing wild-type, GTP-bound/Q77L, GDP-bound/N132I, or sumo-deficient/K68R rab17 were surface labeled for plgA-R or APN for 30 min at 4°C. Cells were additionally infected with recombinant adenoviruses expressing plgA-R. Lysates were immunoblotted with primary antibodies to detect the entire population of plgA-R or APN. On a parallel immunoblot, lysates were probed directly with secondary antibodies to detect only the surface-bound primary antibodies. The amount of surface-bound antibodies was normalized to the total antigen amount. In all cases, control ratios were set to 100%. Values are expressed as the mean  $\pm$  SEM from at least three independent experiments. (D) Total cell lysates were prepared from uninfected (con) WIF-B cells or cells expressing WT, GTP-bound/Q77L, GDP-bound/N132I rab17, or sumo-deficient K68R rab17 and immunoblotted for APN or plgA-R as indicated. In E, cells expressing wild-type, GTP-bound/Q77L, GDP-bound/N132I, or sumo-deficient K68R rab17 were labeled for HA321. Asterisks mark selected bile canaliculi. Bar = 10  $\mu$ m.

buffer. Cleared lysates were mixed with GTP-agarose for 2 h at 4°C. Bound fractions were recovered, washed, and immunoblotted for rab17 using anti-FLAG epitope antibodies. The monosumoylated form of rab17 is indicated with an arrow. Molecular-weight markers are indicated on the left of each immunoblot in kDa. A representative immunoblot from three independent experiments is shown.

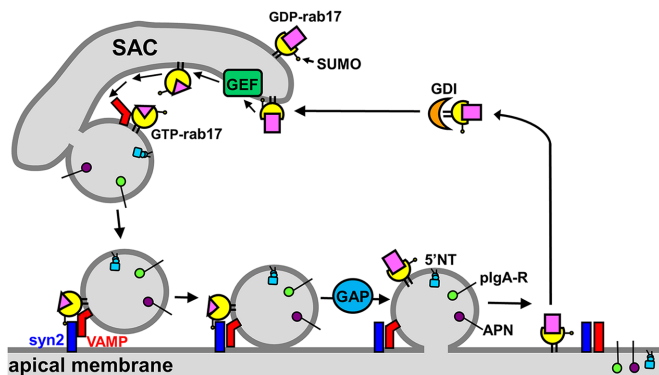


**FIGURE 8:** Model for the role of rab17 in regulation of apical vesicle docking and fusion. The prenylated, monosumoylated, and GDP-bound rab17 is activated by its specific GEF at the SAC. The GTP-bound rab17 associates with a budding vesicle via associations with a transcytotic vesicle-specific VAMP or a yet-to-be-identified coat protein (not shown). The budded vesicle is delivered to the apical membrane where the GTP-bound, sumoylated rab17 interacts with syntaxin 2 to initiate vesicle docking. A rab17-specific GAP at the apical surface activates GTP hydrolysis required for vesicle fusion. The GDP-bound, sumoylated rab17 is extracted from the apical membrane by a GDI and recycled to the SAC. GAP, GTPase-activating protein; GEF, guanine exchange factor; syn2, syntaxin 2; VAMP.

rab GTPases that includes rabs 5A-C, 17, 22A-B, and 31. All family members show a preference for Vps9-domain containing GEFs (Ishida *et al.*, 2016). Of the 10 identified Vps9 GEFs, rabex-5 has been shown to function as a rab17 GEF in hippocampal neurons where it mediates rab17-regulated cargo delivery to developing dendrites and dendritic spines (Mori *et al.*, 2012, 2013; Ishida *et al.*, 2016). Because rabex-5 is also expressed in liver (Horiuchi *et al.*, 1997), it is a good candidate for the hepatic rab17 GEF involved in transcytosis. Of the more than 40 mammalian TBC (Treb2/Bub2/Cdc16)-domain containing rab GAPs (Fukuda, 2011), TBC1D7 has been shown to function as a rab17 GAP in cilia formation in retinal pigment epithelium (Yoshimura *et al.*, 2007). As for rabex-5, TBC1D7 is expressed in rat liver and is a good candidate for the transcytotic hepatic rab17 GAP. We are currently initiating studies to identify the rab17 regulators involved in apical vesicle delivery.

### Rab17 function in transcytosis varies among polarized epithelial cell types

We determined that plgA-R transcytosis in cells expressing wild-type rab17 was indistinguishable from that observed in uninfected control cells. In contrast, wild-type rab17 expression *impaired* basolateral-to-apical plgA-R transcytosis in MDCK cells (Hunziker and Peters, 1998). In mammary gland-derived Eph4 cells expressing GTP-bound or GDP-bound rab17, basolateral-to-apical transcytosis was *enhanced*, whereas we found that expression of either *impaired* transcytosis in polarized WIF-B cells (Zacchi *et al.*, 1998). These conflicting results may be explained by cell type specificity in the expression and distributions of rab17-specific GEFs and GAPs. However, another intriguing possibility is varying degrees of rab17 sumoylation among cell types. By monitoring the modification's appearance in WIF-B cells early after infection, we noticed that modified rab17 appeared with the same kinetics as the unmodified form, but the relative amounts of the sumoylated rab17 to total rab17 remained constant (at 35–40%), suggesting that sumoylation is reversible (Striz and Tuma, 2016). Similarly, the proportions remained

constant in cells treated with cycloheximide, and both species were degraded with identical kinetics (Striz and Tuma, 2016). Thus, not only is the modification reversible, it is maintained at very specific steady-state levels. How this is regulated and what it signifies is not clear, but it may well vary among cell types and explain the disparate observations. Also interesting is the finding that rab17 prenylation is required for sumoylation (Striz and Tuma, 2016). Again, the significance of this finding is not clear but may represent sumoylation ligase(s) specificity in rab17 binding interactions among cell types. Further studies are clearly needed to sort this out.

### Rab17 sumoylation on lysine 68 enhances its function in apical vesicle docking

From our earlier studies, we identified and mutated two near-perfect sumoylation consensus sites at lysines 41 and 68 to arginines alone or in combination. Only the K68R point mutant decreased rab17 sumoylation (the double mutant did not fold properly), suggesting that it is the important lysine (Striz and Tuma, 2016). Although not completely abolished, a reproducible and statistically significant 30% decrease in K68R sumoylation was observed, which was consistent with the 30% decrease in wild-type rab17 sumoylation we observed after SENP1 cleavage (Striz and Tuma, 2016). Although treatment with anacardic acid led to a ~60% decrease of rab17 sumoylation, it did not further inhibit transcytosis in K68R rab17-expressing cells. At present, we cannot account for the remaining levels of sumoylation observed on the mutant after anacardic acid treatment. Similar results have been reported for single-site lysine mutants in other known nonnuclear sumoylated proteins (Fuhs and Insel, 2011; Gonzalez-Santamaria *et al.*, 2012; Qu *et al.*, 2014; Caron *et al.*, 2015), and some have argued that these incomplete losses can be explained by the presence of nonspecific sumoylation at nonconventional or cryptic sites. Thus, we propose that lysine 68 is the important sumoylated residue for rab17 optimal function in apical vesicle docking and fusion.

### Clinical implications of our findings

In the past few years, it has become apparent that rab17 expression is significantly decreased in epithelial-derived human gastric cancer and in hepatocellular carcinoma (HCC) (Aquea *et al.*, 2014; Qi *et al.*, 2015; Wang *et al.*, 2015). Recent studies have revealed that 75% of patient paraneoplastic liver tissue samples express rab17, whereas only 35% of HCC patient samples did (Wang *et al.*, 2015). This decreased rab17 expression can be explained by studies in breast cancer cells where extracellular signal-regulated kinase (ERK)-activated alterations in gene expression led to decreased rab17 expression (von Thun *et al.*, 2012; Qi *et al.*, 2015; Wang *et al.*, 2015). Additionally, overexpression of rab17 in HCC cell lines ameliorated the tumorigenic phenotype while its knockdown enhanced invasiveness consistent with its role as a tumor suppressor (Qi *et al.*, 2015; Wang *et al.*, 2015). The clinical relevance of these findings highlights the obvious need for the further examination and identification of the mechanisms by which rab17 functions in apical protein sorting and/or trafficking in liver health and disease. Such information will better inform our interpretation of phenotypes observed in other epithelial-derived cancerous cells and lead to unique therapeutic strategies and targets.

## MATERIALS AND METHODS

### Reagents and antibodies

F12 (Coon's modification) medium, horseradish peroxidase (HRP)-conjugated secondary antibodies and monoclonal antibodies against the FLAG epitope were purchased from Sigma-Aldrich

(St. Louis, MO). HEPES and Alexa-466 and -568-conjugated secondary antibodies were purchased from Life Technologies (Carlsbad, CA). Anacardic acid was from Enzo Life Sciences (Farmingdale, NY). Monoclonal antibodies against the V5 epitope tag or full-length rab17 were from AbD Serotec (Raleigh, NC) and Proteintech (Chicago, IL), respectively. Monoclonal antibodies against EEA1 were from BD Biosciences (San Jose, CA). Fetal bovine serum (FBS) was from Gemini Bio-Products (Woodland, CA). Monoclonal antibodies against the myc epitope (9E10), 5'NT, endolyn-78 and HA321 were kindly provided by Ann Hubbard (Johns Hopkins University School of Medicine, Baltimore, MD) and have been described previously (Hubbard *et al.*, 1985; Schell *et al.*, 1992; Ihrke *et al.*, 1998; Bastaki *et al.*, 2002). Polyclonal antibodies against APN, ASGP-R, albumin, and syntaxin 2 were also provided by Ann Hubbard and have been described previously (Bartles *et al.*, 1985a,b; Fujita *et al.*, 1998; Ihrke *et al.*, 1998). These antibodies are all now part of our permanent stocks.

### Cell culture

WIF-B cells were grown in a humidified 7% CO<sub>2</sub> incubator at 37°C as described (Shanks *et al.*, 1994). Briefly, cells were grown in F12 medium (Coon's modification), pH 7.0, supplemented with 5% FBS, 10 μM hypoxanthine, 40 nM aminoterpin, and 1.6 μM thymidine. WIF-B cells were seeded onto glass coverslips at 1.3 × 10<sup>4</sup> cells/cm<sup>2</sup> and cultured for 8–12 d until they reached maximal density and polarity. Cells are routinely tested for mycoplasma contamination.

### Virus production and infection

Recombinant adenoviruses encoding N-terminally myc or FLAG-tagged full-length wild-type, GTP-bound/Q77L, GDP-bound/N132I rab17, or sumo-deficient/K68R mutant rab17 were generated using the ViraPower Adenoviral Expression System (Life Technologies) as described (Striz and Tuma, 2016). Recombinant adenoviruses encoding full-length myc-tagged plgA-R have been described previously (Bastaki *et al.*, 2002). WIF-B cells were infected with recombinant adenovirus particles for 60 min at 37°C as described (Bastaki *et al.*, 2002). Complete medium was added to the cells and they were incubated an additional 16–24 h to allow for protein expression.

### Immunoblotting

Samples were mixed with Laemmli sample buffer (Laemmli, 1970) and boiled for 3 min. Proteins were electrophoretically separated using SDS-PAGE, transferred to nitrocellulose using a Transblot Turbo (BioRad, Hercules, CA), and immunoblotted with the indicated antibodies. HRP-conjugated secondary antibodies were used at 5 ng/ml, and immunoreactivity was detected with enhanced chemiluminescence (PerkinElmer, Waltham, MA) using the ChemiDoc Touch Imager (BioRad). Relative protein levels were determined by densitometric analysis of immunoreactive bands using the ChemiDoc imaging software or ImageJ software (National Institutes of Health).

### Immunofluorescence microscopy and imaging

In general, control or infected cells were fixed on ice with chilled phosphate-buffered saline (PBS) containing 4% paraformaldehyde for 1 min and permeabilized with ice-cold methanol for 10 min or fixed with ice-cold methanol for 5 min at -20°C. Cells were processed for indirect immunofluorescence as previously described (Ihrke *et al.*, 1993). Alexa 488- or 568-conjugated secondary antibodies were used at 3–5 μg/ml. Labeled cells were visualized at room temperature by epifluorescence with an Olympus BX60 Fluorescence Microscope (OPELCO, Dulles, VA) using an UPlanFl 60x/NA 1.3, phase 3, oil immersion objective. Images were taken with an HQ2 CoolSnap digital camera (Roper Scientific, Germany) using IP Labs software (BD

Biosciences, Rockville, MD) or MetaMorph software (Molecular Devices, Sunnyvale, CA). Adobe Photoshop (Adobe Systems, Mountain View, CA) was used to process images and to compile figures.

To determine Mander's coefficients of colocalization, at least five fields were imaged using a 60x objective. Regions of interest (ROIs) placed at the apical domain and immediate surrounding area were selected to exclude nonpolarized and noninfected cells from the analysis and to exclude residual basolateral labeling from the analysis. In general, 5–10 fields per condition were imaged with each field having 10–30 apical domains. Values presented in figures were calculated from at least three independent experiments.

### Antibody trafficking in live cells

We monitored transcytosis with an assay we previously developed (Ihrke *et al.*, 1998; In *et al.*, 2012). Briefly, uninfected WIF-B cells or cells expressing wild-type, GTP-bound/Q77L, GDP-bound/N132I, or sumo-deficient/K68R rab17 were basolaterally labeled with antibodies specific to APN (1:50), 5'NT (1:50) or myc (1:100; to label plgA-R) for 20 min at 4°C. Cells were washed three times for 2 min on ice and then reincubated with prewarmed complete medium. Antibody-antigen complexes were chased for 0, 45, or 90 min (for 5'NT) or 0, 30, and 60 min (for APN and plgA-R) at 37°C and processed for immunofluorescence labeling. Cells were pretreated with 5 μM anacardic acid for 60 min at 37°C before antibody labeling, and the assay was performed in the continued presence of the drug. To semi-quantitate apical delivery, we used a method we developed over 10 years ago and have used extensively (Ramnarayanan *et al.*, 2007; In and Tuma, 2010; In *et al.*, 2012, 2014; Groebner *et al.*, 2014). From micrographs, the average pixel intensity of selected ROI placed at the apical or basolateral membrane of the same WIF-B cell (to control for expression level differences) were measured using the Measure ROI tool of the ImageJ imaging software (National Institutes of Health, Bethesda, MD). In general, multiple ROI were collected in the same cell to verify that representative intensities were measured. The averaged background pixel intensity (taken over the nucleus) was subtracted from each value, and the ratio of apical-to-basolateral membrane fluorescence intensity was determined. In general, 5–10 fields are imaged using a 60x objective with each field having 10–30 apical domains. Because each apical canalicular domain is formed by at least two cells, each domain has two measurements. Thus, hundreds of ratio measurements are performed per time point per experiment. Values presented in figures were calculated from at least three independent experiments.

To identify the subapical compartment with accumulated cargo, cells were continuously labeled from the basolateral surface with antibodies against 5'NT and ASGP-R (to identify basolateral early endosomes) or against APN and endolyn-78 (to mark the SAC) (Ihrke *et al.*, 1998) for 60 min at 37°C using previously published methods (Ihrke *et al.*, 1998; In *et al.*, 2012). Cells were washed three times for 2 min with prewarmed complete medium and processed for epifluorescence imaging. Alternatively, after 60 min of chase with 5'NT- or APN-specific antibodies as indicated, cells were fixed and labeled for steady-state distributions of syntaxin 2 or EEA1. Images were merged and Mander's coefficients of colocalization were determined.

### GTP pull downs

Uninfected WIF-B cells or cells expressing wild-type or K68R rab17 were scraped into ice-cold GTP binding buffer (TBS, pH 7.4, containing 5 mM MgCl<sub>2</sub> and 1% [vol/vol] Triton X-100) plus added protease inhibitors. Cells were lysed on ice for 30 min, and the lysates were cleared by centrifugation for 10 min at 10,000 × *g* at 4°C. A 50% slurry of GTP-agarose (Sigma Aldrich) was added to each tube,

and the tubes were rotated for 2 h at 4°C. The bound proteins were recovered by centrifugation at 2000 rpm at 4°C for 2 min. The bound samples were washed three times with GTP binding buffer and recovered by centrifugation as above. Final pelleted samples were lysed directly in Laemmli sample buffer and processed for immunoblotting for rab17 using anti-FLAG epitope antibodies.

### Basolateral secretion

Control or infected cells were rinsed five times with prewarmed serum-free medium and then reincubated in serum-free medium. At 0, 15, 30, and 60 min after reincubation, aliquots of media were collected and analyzed for albumin secretion by immunoblotting and densitometric analysis of immunoreactive bands as we have previously described (Joseph *et al.*, 2007; In *et al.*, 2014).

### Basolateral delivery

To monitor basolateral delivery, we used an assay that we previously developed (Ramnarayanan *et al.*, 2007; In *et al.*, 2012). Briefly, WIB cells were infected with wild-type, GTP-bound/Q77L, GDP-bound/N132I, or sumo-deficient/K68R rab17 for 20 h. Cells were incubated with antibodies to externally exposed antigens of either APN or pIgA-R on ice for 20 min and lysed by addition of Laemmli sample buffer. Lysates were immunoblotted with APN or pIgA-R antibodies to detect the entire population of each apical resident. On a parallel immunoblot, lysates were probed directly with secondary antibodies to detect only the surface bound primary antibodies. The relative levels of immunoreactive species were determined by densitometry. The amount of surface-bound antibodies was normalized to the amount of total antigen present. In all cases, control ratios were set to 100%.

### Statistical analysis

Results are expressed as the mean  $\pm$  SEM from at least three independent experiments. Comparisons between experimental groups were made using the Student's two-tailed *t* test for paired data. *P* values  $\leq 0.05$  were considered significant.

## ACKNOWLEDGMENTS

We thank Ann Hubbard (Johns Hopkins University School of Medicine) for providing the many antibodies and viruses used in these studies. This work was supported by National Institutes of Health Grant R01 DK082890 awarded to P.L.T.

## REFERENCES

Alvarez C, Fujita H, Hubbard A, Sztul E (1999). ER to Golgi transport: Requirement for p115 at a pre-Golgi VTC stage. *J Cell Biol* 147, 1205–1222.

Aquea G, Bresky G, Lancellotti D, Madariaga JA, Zaffiri V, Urzua U, Haberle S, Bernal G (2014). Increased expression of P2RY2, CD248 and EphB1 in gastric cancers from Chilean patients. *Asian Pac J Cancer Prev* 15, 1931–1936.

Barr VA, Hubbard AL (1993). Newly synthesized hepatocyte plasma membrane proteins are transported in transcytotic vesicles in the bile duct-ligated rat. *Gastroenterology* 105, 554–571.

Bartles JR, Braiterman LT, Hubbard AL (1985a). Biochemical characterization of domain-specific glycoproteins of the rat hepatocyte plasma membrane. *J Biol Chem* 260, 12792–12802.

Bartles JR, Braiterman LT, Hubbard AL (1985b). Endogenous and exogenous domain markers of the rat hepatocyte plasma membrane. *J Cell Biol* 100, 1126–1138.

Bartles JR, Feracci HM, Stieger B, Hubbard AL (1987). Biogenesis of the rat hepatocyte plasma membrane in vivo: comparison of the pathways taken by apical and basolateral proteins using subcellular fractionation. *J Cell Biol* 105, 1241–1251.

Bartles JR, Hubbard AL (1988). Plasma membrane protein sorting in epithelial cells: do secretory pathways hold the key? *Trends Biochem Sci* 13, 181–184.

Bastaki M, Braiterman LT, Johns DC, Chen YH, Hubbard AL (2002). Absence of direct delivery for single transmembrane apical proteins or their "Secretory" forms in polarized hepatic cells. *Mol Biol Cell* 13, 225–237.

Beaumont KA, Hamilton NA, Moores MT, Brown DL, Ohbayashi N, Cairncross O, Cook AL, Smith AG, Misaki R, Fukuda M, *et al.* (2011). The recycling endosome protein Rab17 regulates melanocytic filopodia formation and melanosome trafficking. *Traffic* 12, 627–643.

Biagini CP, Boissel E, Borde F, Bender VE, Bouskila M, Blazy F, Nicaise L, Mignot A, Cassio D, Chevalier S (2006). Investigation of the hepatotoxicity profile of chemical entities using Liverbeads and WIF-B9 in vitro models. *Toxicol In Vitro* 20, 1051–1059.

Caron D, Boutchueng-Djidjou M, Tanguay RM, Faure RL (2015). Annexin A2 is SUMOylated on its N-terminal domain: regulation by insulin. *FEBS Lett* 589, 985–991.

Chaumontet C, Mazzoleni G, Decaens C, Bex V, Cassio D, Martel P (1998). The polarized hepatic human/rat hybrid WIF 12-1 and WIF-B cells communicate efficiently in vitro via connexin 32-constituted gap junctions. *Hepatology* 28, 164–172.

De Marco MC, Martin-Belmonte F, Kremer L, Albar JP, Correas I, Vaerman JP, Marazuela M, Byrne JA, Alonso MA (2002). MAL2, a novel raft protein of the MAL family, is an essential component of the machinery for transcytosis in hepatoma HepG2 cells. *J Cell Biol* 159, 37–44.

Folmer DE, van der Mark VA, Ho-Mok KS, Oude Elferink RP, Paulusma CC (2009). Differential effects of progressive familial intrahepatic cholestasis type 1 and benign recurrent intrahepatic cholestasis type 1 mutations on canalicular localization of ATP8B1. *Hepatology* 50, 1597–1605.

Fuhs SR, Insel PA (2011). Caveolin-3 undergoes SUMOylation by the SUMO E3 ligase PIASy: sumoylation affects G-protein-coupled receptor desensitization. *J Biol Chem* 286, 14830–14841.

Fujita H, Tuma PL, Finnegan CM, Locco L, Hubbard AL (1998). Endogenous syntaxins 2, 3 and 4 exhibit distinct but overlapping patterns of expression at the hepatocyte plasma membrane. *Biochem J* 329, 527–538.

Fukuda M (2011). TBC proteins: GAPs for mammalian small GTPase Rab? *Biosci Rep* 31, 159–168.

Gao J, Chen J, Heremity M, Tsukamoto H, Zhang AS, Enns CA (2009). Interaction of the hereditary hemochromatosis protein HFE with transferrin receptor 2 is required for transferrin-induced hepcidin expression. *Cell Metab* 9, 217–227.

Garuti R, Jones C, Li WP, Michael P, Herz J, Gerard RD, Cohen JC, Hobbs HH (2005). The modular adaptor protein autosomal recessive hypercholesterolemia (ARH) promotes low density lipoprotein receptor clustering into clathrin-coated pits. *J Biol Chem* 280, 40996–41004.

Gonzalez-Santamaria J, Campagna M, Ortega-Molina A, Marcos-Villar L, de la Cruz-Herrera CF, Gonzalez D, Gallego P, Lopitz-Otsoa F, Esteban M, Rodriguez MS, *et al.* (2012). Regulation of the tumor suppressor PTEN by SUMO. *Cell Death Dis* 3, e393.

Gradilone SA, Tietz PS, Splinter PL, Marinelli RA, LaRusso NF (2005). Expression and subcellular localization of aquaporin water channels in the polarized hepatocyte cell line, WIF-B. *BMC Physiol* 5, 13.

Graf GA, Yu L, Li WP, Gerard R, Tuma PL, Cohen JC, Hobbs HH (2003). ABCG5 and ABCG8 are obligate heterodimers for protein trafficking and biliary cholesterol excretion. *J Biol Chem* 278, 48275–48282.

Groebner JL, Fernandez DJ, Tuma DJ, Tuma PL (2014). Alcohol-induced defects in hepatic transcytosis may be explained by impaired dynein function. *Mol Cell Biochem* 397, 223–233.

Harder CJ, Meng A, Rippstein P, McBride HM, McPherson R (2007). SR-BI undergoes cholesterol-stimulated transcytosis to the bile canaliculus in polarized WIF-B cells. *J Biol Chem* 282, 1445–1455.

Hayes JH, Soroka CJ, Rios-Velez L, Boyer JL (1999). Hepatic sequestration and modulation of the canalicular transport of the organic cation, daunorubicin, in the Rat. *Hepatology* 29, 483–493.

Horiuchi H, Lippe R, McBride HM, Rubino M, Woodman P, Stenmark H, Rybin V, Wilm M, Ashman K, Mann M, Zerial M (1997). A novel Rab5 GDP/GTP exchange factor complexed to Rabaptin-5 links nucleotide exchange to effector recruitment and function. *Cell* 90, 1149–1159.

Hubbard AL, Bartles JR, Braiterman LT (1985). Identification of rat hepatocyte plasma membrane proteins using monoclonal antibodies. *J Cell Biol* 100, 1115–1125.

Hunziker W, Peters PJ (1998). Rab17 localizes to recycling endosomes and regulates receptor-mediated transcytosis in epithelial cells. *J Biol Chem* 273, 15734–15741.

Ihrke G, Martin GV, Shanks MR, Schrader M, Schroer TA, Hubbard AL (1998). Apical plasma membrane proteins and endolyn-78 travel through a subapical compartment in polarized WIF-B hepatocytes. *J Cell Biol* 141, 115–133.

- Ihrke G, Neufeld EB, Meads T, Shanks MR, Cassio D, Laurent M, Schroer TA, Pagano RE, Hubbard AL (1993). WIF-B cells: an in vitro model for studies of hepatocyte polarity. *J Cell Biol* 123, 1761–1775.
- In JG, Ihrke G, Tuma PL (2012). Analysis of polarized membrane traffic in hepatocytes and hepatic cell lines. *Curr Protoc Cell Biol* Chapter 15, Unit 15 17.
- In JG, Striz AC, Bernad A, Tuma PL (2014). Serine/threonine kinase 16 and MAL2 regulate constitutive secretion of soluble cargo in hepatic cells. *Biochem J* 463, 201–213.
- In JG, Tuma PL (2010). MAL2 selectively regulates polymeric IgA receptor delivery from the Golgi to the plasma membrane in WIF-B cells. *Traffic* 11, 1056–1066.
- Ishida M, M EO, Fukuda M (2016). Multiple types of guanine nucleotide exchange factors (GEFs) for Rab small GTPases. *Cell Struct Funct* 41, 61–79.
- Jin M, Saucan L, Farquhar MG, Palade GE (1996). Rab1a and multiple other Rab proteins are associated with the transcytotic pathway in rat liver. *J Biol Chem* 271, 30105–30113.
- Joseph RA, Shepard BD, Kannarkat GT, Rutledge TM, Tuma DJ, Tuma PL (2007). Microtubule acetylation and stability may explain alcohol-induced alterations in hepatic protein trafficking. *Hepatology* 47, 1745–1753.
- Laemmli UK (1970). Cleavage of structural proteins during the assembly of the head of bacteriophage T4. *Nature* 227, 680–685.
- Lehtonen S, Lehtonen E, Olkkonen VM (1999). Vesicular transport and kidney development. *Int J Dev Biol* 43, 425–433.
- Leitch S, Feng M, Muend S, Braiterman LT, Hubbard AL, Rao R (2010). Vesicular distribution of Secretory Pathway Ca<sup>2+</sup>-ATPase isoform 1 and a role in manganese detoxification in liver-derived polarized cells. *Biometals* 24, 159–170.
- Lionne C, Buss F, Hodge T, Ihrke G, Kendrick-Jones J (2001). Localization of myosin Va is dependent on the cytoskeletal organization in the cell. *Biochem Cell Biol* 79, 93–106.
- Lutcke A, Jansson S, Parton RG, Chavrier P, Valencia A, Huber LA, Lehtonen E, Zerial M (1993). Rab17, a novel small GTPase, is specific for epithelial cells and is induced during cell polarization. *J Cell Biol* 121, 553–564.
- McVicker BL, Rasineni K, Tuma DJ, McNiven MA, Casey CA (2012). Lipid droplet accumulation and impaired fat efflux in polarized hepatic cells: consequences of ethanol metabolism. *Int J Hepatol* 2012, 978136.
- McVicker BL, Tuma PL, Kharbanda KK, Lee SM, Tuma DJ (2009). Relationship between oxidative stress and hepatic glutathione levels in ethanol-mediated apoptosis of polarized hepatic cells. *World J Gastroenterol* 15, 2609–2616.
- Meads T, Schroer TA (1995). Polarity and nucleation of microtubules in polarized epithelial cells. *Cell Motil Cytoskeleton* 32, 273–288.
- Mori Y, Matsui T, Fukuda M (2013). Rabex-5 protein regulates dendritic localization of small GTPase Rab17 and neurite morphogenesis in hippocampal neurons. *J Biol Chem* 288, 9835–9847.
- Mori Y, Matsui T, Furutani Y, Yoshihara Y, Fukuda M (2012). Small GTPase Rab17 regulates dendritic morphogenesis and postsynaptic development of hippocampal neurons. *J Biol Chem* 287, 8963–8973.
- Neufeld EB, Demosky SJ Jr, Stonik JA, Combs C, Remaley AT, Duverger N, Santamarina-Fojo S, Brewer HB Jr (2002). The ABCA1 transporter functions on the basolateral surface of hepatocytes. *Biochem Biophys Res Commun* 297, 974–979.
- Nyasae LK, Hubbard AL, Tuma PL (2003). Transcytotic efflux from early endosomes is dependent on cholesterol and glycosphingolipids in polarized hepatic cells. *Mol Biol Cell* 14, 2689–2705.
- Nyasae LK, Schell MJ, Hubbard AL (2014). Copper directs ATP7B to the apical domain of hepatic cells via basolateral endosomes. *Traffic* 15, 1344–1365.
- Paulusma CC, Folmer DE, Ho-Mok KS, de Waart DR, Hilarius PM, Verhoeven AJ, Oude Elferink RP (2008). ATP8B1 requires an accessory protein for endoplasmic reticulum exit and plasma membrane lipid flippase activity. *Hepatology* 47, 268–278.
- Peters PJ, Hunziker W (2001). Subcellular localization of Rab17 by cryo-immunogold electron microscopy in epithelial cells grown on polycarbonate filters. *Methods Enzymol* 329, 210–225.
- Pujol AM, Cuillel M, Renaudet O, Lebrun C, Charbonnier P, Cassio D, Gateau C, Dumy P, Mintz E, Delangle P (2011). Hepatocyte targeting and intracellular copper chelation by a thiol-containing glycoconjugate. *J Am Chem Soc* 133, 286–296.
- Qi J, Zhao P, Li F, Guo Y, Cui H, Liu A, Mao H, Zhao Y, Zhang X (2015). Down-regulation of Rab17 promotes tumorigenic properties of hepatocellular carcinoma cells via Erk pathway. *Int J Clin Exp Pathol* 8, 4963–4971.
- Qu Y, Chen Q, Lai X, Zhu C, Chen C, Zhao X, Deng R, Xu M, Yuan H, Wang Y, et al. (2014). SUMOylation of Grb2 enhances the ERK activity by increasing its binding with Sos1. *Mol Cancer* 13, 95.
- Ramnarayanan SP, Cheng CA, Bastaki M, Tuma PL (2007). Exogenous MAL reroutes selected hepatic apical proteins into the direct pathway in WIF-B cells. *Mol Biol Cell* 18, 2707–2715.
- Schaffert CS, Todero SL, McVicker BL, Tuma PL, Sorrell MF, Tuma DJ (2004). WIF-B cells as a model for alcohol-induced hepatocyte injury. *Biochem Pharmacol* 67, 2167–2174.
- Schell MJ, Maurice M, Stieger B, Hubbard AL (1992). 5′nucleotidase is sorted to the apical domain of hepatocytes via an indirect route [published erratum appears in *J Cell Biol* 1993 Nov;123(3): following 767]. *J Cell Biol* 119, 1173–1182.
- Shanks MS, Cassio D, Lecoq O, Hubbard AH (1994). An improved rat hepatoma hybrid cell line. Generation and comparison with its hepatoma relatives and hepatocytes in vivo. *J Cell Sci* 107, 813–825.
- Striz AC, Tuma PL (2016). The GTP-bound and sumoylated form of the rab17 small molecular weight GTPase selectively binds Syntaxin 2 in polarized hepatic WIF-B cells. *J Biol Chem* 291, 9721–9732.
- Sturm E, Zimmermann TL, Crawford AR, Svetlov SI, Sundaram P, Ferrara JL, Karpen SJ, Crawford JM (2000). Endotoxin-stimulated macrophages decrease bile acid uptake in WIF-B cells, a rat hepatoma hybrid cell line. *Hepatology* 31, 124–130.
- Suda J, Rockey DC, Karvar S (2015). Akt2-dependent phosphorylation of radixin in regulation of Mrp-2 trafficking in WIF-B cells. *Dig Dis Sci* 61, 453–463.
- Tuma P, Hubbard A (2001). The hepatocyte surface: dynamic polarity. In: *The Liver: Biology and Pathology*, ed. I Arias, J Boyer, F Chisari, N Fausto, D Schachter, and D Shafritz, Philadelphia: Lippincott Williams and Wilkins, 97–117.
- Tuma PL, Finnegan CM, Yi JH, Hubbard AL (1999). Evidence for apical endocytosis in polarized hepatic cells: phosphoinositide 3-kinase inhibitors lead to the lysosomal accumulation of resident apical plasma membrane proteins. *J Cell Biol* 145, 1089–1102.
- Tuma PL, Hubbard AL (2003). Transcytosis: crossing cellular barriers. *Physiol Rev* 83, 871–932.
- Tuma PL, Nyasae LK, Backer JM, Hubbard AL (2001). Vps34p differentially regulates endocytosis from the apical and basolateral domains in polarized hepatic cells. *J Cell Biol* 154, 1–13.
- Tuma PL, Nyasae LK, Hubbard AL (2002). Nonpolarized cells selectively sort apical proteins from cell surface to a novel compartment, but lack apical retention mechanisms. *Mol Biol Cell* 13, 3400–3415.
- von Thun A, Birtwistle M, Kalna G, Grindlay J, Strachan D, Kolch W, von Kriegsheim A, Norman JC (2012). ERK2 drives tumour cell migration in three-dimensional microenvironments by suppressing expression of Rab17 and liprin-beta2. *J Cell Sci* 125, 1465–1477.
- Wakabayashi Y, Dutt P, Lippincott-Schwartz J, Arias IM (2005). Rab11a and myosin Vb are required for bile canalicular formation in WIF-B9 cells. *Proc Natl Acad Sci USA* 102, 15087–15092.
- Wang K, Mao Z, Liu L, Zhang R, Liang Q, Xiong Y, Yuan W, Wei L (2015). Rab17 inhibits the tumorigenic properties of hepatocellular carcinomas via the Erk pathway. *Tumour Biol* 36, 5815–5824.
- Yoshimura S, Egerer J, Fuchs E, Haas AK, Barr FA (2007). Functional dissection of Rab GTPases involved in primary cilium formation. *J Cell Biol* 178, 363–369.
- Zacchi P, Stenmark H, Parton RG, Orioli D, Lim F, Giner A, Mellman I, Zerial M, Murphy C (1998). Rab17 regulates membrane trafficking through apical recycling endosomes in polarized epithelial cells. *J Cell Biol* 140, 1039–1053.